Mon. Not. R. Astron. Soc. **000**, 1–14 (2011)   Printed 10 October 2011   (MN LaTeX style file v2.2)

arXiv:1110.1396v1 [astro-ph.SR] 6 Oct 2011

Thermally Pulsing Asymptotic Giant Branch Star Models and Globular Cluster Planetary Nebulae I: The Model

J. F. Buell[1]*
[1] *100 College Drive, SUNY College of Technology at Alfred, Alfred, NY 14843, USA*

10 October 2011

ABSTRACT

Thermally pulsing asymptotic giant branch models of globular cluster stars are calculated using a synthetic model with the goal of reproducing the chemical composition, core masses and other observational parameters of the four known globular cluster planetary nebulae as well as roughly matching the overall cluster properties. The evolution of stars with an enhanced helium abundance (Y) and blue stragglers are modeled. New pre-thermally pulsing asymptotic giant branch mass-losses for red giant branch and early asymptotic giant branch stars are calculated from the Padova stellar evolution models (Bertelli et al. 2008, 2009). The new mass-losses are calculated to get the relative differences in mass-losses due to enhanced helium abundances.

The global properties of the globular cluster planetary nebula are reproduced with these models. The metallicity, mass of the central star, overall metallicities, helium abundance and the nebular mass are matched to the observational values. Globular cluster planetary nebulae JaFu 1 and JaFu 2 are reproduced *by assuming progenitor stars* with masses near the typical main sequence turn-offs of globular clusters and with enhanced helium abundances very similar to the enhancements inferred from fitting isochrones to globular cluster colour-magnitude diagrams. The globular cluster PN GJJC-1 can be roughly fit by a progenitor star with very extreme helium enhancement ($Y \approx 0.40$) near the turn-off producing a central star with the same mass as inferred by observations and a very low nebular mass. The abundances and core mass of planetary nebula Ps 1 and its central star (K648) are reproduced by a blue straggler model. However, it turned out to be impossible to reproduce its nebular mass and it is concluded some kind of binary scenario may be needed to explain K648.

Key words: stars:AGB and post-AGB – blue stragglers - mass-loss – white dwarfs – globular clusters: general – planetary nebulae: individual

1 INTRODUCTION

The globular cluster (GC) system of the Galaxy contains four known planetary nebulae (PNe) all of which have unusual abundances. The nebulae Ps 1 and its central star K648 in M15 have a very high C/O ratio of nearly 10 (Alves et al. 2000; Bianchi et al. 1995, 2001; Howard et al. 1997; Rauch et al. 2002). The PNe JaFu 1 in Pal 6 and JaFu 2 in NGC 6441 have high ratios of He/H (Jacoby et al. 1997) (0.115 and 0.141 for JaFu 1 and JaFu 2, respectively). The fourth GC PN GJJC-1 in M22 is one of three known PN with no hydrogen in the nebula (Jacoby et al. 1997). All four are very different from the typical disc PN. They are even more difficult to explain since the typical age of a globular cluster is $\sim 12.5\,\mathrm{Gyr}$ leading to a turn-off mass of $\sim 0.85\,\mathrm{M}_{\odot}$. At this mass only minor changes from the zero-age main sequence (ZAMS) abundances to PN abundances are expected. If the progenitors had a typical halo or thick disc compositon the abundance ratios would be similar to those found in disk PNe (He/H~ 0.100, C/O< 1 and N/O~ 0.4). The origin of these PNe requires an explanation.

Jacoby et al. (1997) surveyed 130 GCs in a search for PN in GC. They concluded that the number known is probably complete. They found this is less than the expected number (≈ 16) given the total luminosity of the Galactic globular cluster system. This number is based on stellar populations which are younger than the stars in globular clusters. GCs have very low mass turn-offs ($\sim 0.85\,\mathrm{M}_{\odot}$). At this mass a typical PN central star (CSPN) should have a mass of $\sim 0.52\,\mathrm{M}_{\odot}$. The time required from when a star of this mass leaves the asymptotic giant branch (AGB) for this star to get hot enough to ionize the ejected mass would be

---

* E-mail: buelljf@alfredstate.edu

too long. The ejected mass would dissipate before a visible PN could be observed. This is known as a “lazy” planetary nebula (Renzini 1979).

The masses of the central stars of the globular cluster PN are larger than the typical measured masses of the youngest white dwarfs (WDs) at the top of the cooling sequence. The cooling sequences of white dwarfs in globular clusters have been determined by a number of authors (Renzini et al. 1996; Cool, Piotto & King 1996; Richer et al. 1997; Zoccali et al. 2001; Hansen et al. 2002, 2004, 2007; Calamida et al. 2008). They find that the majority of main sequence stars evolve into white dwarfs of mass 0.5-0.55 $\mathrm{M}_{\odot}$. and the average of a young GC white dwarf is probably between 0.50 and 0.53 $\mathrm{M}_{\odot}$. All of the GC PNe have central star (CSPN) masses above this average. Alves et al. (2000) and Bianchi et al. (2001) find that the mass of the central star of Ps 1 is 0.58-0.60 $\mathrm{M}_{\odot}$. (Jacoby et al. 1997) determined the CSPN of JaFu 1 and JaFu 2 have masses of 0.55 $\mathrm{M}_{\odot}$. The estimated mass of GJJC-1 is around 0.56 $\mathrm{M}_{\odot}$ (Peña et al. 1992).

Both the CSPN masses higher than the white dwarfs and the unusual abundances seem to require unusual stars as progenitors. GCs contain a variety of unusual star types in addition to the standard types of stars which should be considered as potential progenitors of GC PNe. GCs contain blue stragglers which are thought to be the mergers of two main sequence stars and hence act like main sequence stars with masses higher then the turn-off mass. Bianchi et al. (2001) and Alves et al. (2000) suggested the projenitor of Ps 1 is a blue straggler because of its high core mass and evidence of at least one third dredge up (TDU) event as evidenced by the very high C/O ratio in the nebula. Theoretical models of thermally pulsing-AGB (TP-AGB) stars suggest a core mass of $\sim 0.58\,\mathrm{M}_{\odot}$ is required to get a TDU event.

Another type of star found in globular clusters are second generation stars which incorporate material from the more massive stars of the first generation (primordial component or P). The first generation stars have abundances which reflect the abundances of the interstellar medium material from which they formed and hence have a normal amount of helium ($Y \approx 0.25$). The second generation often incorporates material with a higher fraction of helium than normal ($Y \approx 0.30$). Some clusters show evidence for additional populations with even higher Y values (E.g. Caloi & D’Antona (2007)). These multiple populations show up observationally in a number of ways. It shows up as an Na-O anticorrelation in both red giants and in main sequence stars. This was first observed by Gratton et al. (2001) when they noted the Na-O anticorrelation shows up in main-sequence stars in addition to red giants in several clusters. Some clusters have distinct multiple main sequences (e.g. ωCen (Bedin et al. 2004), NGC 2808 (Piotto et al. 2007), etc.) which can be fit by having a second main sequence with a higher Y. There are GC with multiple subgiant branches (e.g. M22 (Milone et al. 2010a,b), NGC 104, etc.). See Piotto (2009) for a review of the evidence.

These second generation stars form a substantial portion of all stars in GC (up to 60-70 percent of the total number of stars in a GC (Carretta et al. 2009)) and should have a substantial impact on what is observed during the AGB and PN phases of evolution. In this paper I look at the expectations of the PN phase from all the generations of GC stars. I also model the expected PN phase of the blue straggler stars. In section 2 I describe the TP-AGB model used. In section 3 I describe the results of these models. In section 4 I discuss some implications. In section 5 I summarize the results.

2 MODELS

Most of the relevant details of this model are explained in Buell et al. (1997), Buell (1997), and Gavilan, Buell, & Molla (2005). In this section I concentrate on modifications of this model. Of particular importance is the mass-loss on the RGB and E-AGB which can be significant input, especially at the low ZAMS masses of globular cluster stars. Particular attention is paid to the effect of enhanced helium abundances on mass-loss during these stages. The mass-loss in these stages is found by integrating the mass-loss rate formula over the Padua tracks. There is an important point to note, in the pre-TP-AGB mass-loss model the stellar evolution and the mass-loss are not coupled and hence the equations for mass-loss derived below should be used with care. The mass-loss shift is probably a small effect as explained below but the reader should be aware of it.

2.1 Red giant mass-loss

The mass-loss which occurs on the red giant branch (RGB) is very important for low mass stars found in globular clusters, in some extreme cases it may sometimes prevent the star from even reaching the TP-AGB. Most of the pre-TP-AGB mass-loss occurs during the RGB. The standard method to determine the amount of mass-loss is to use Reimers’ Law (Reimers 1975) given by

$$\dot{M} = \eta \frac{LR}{M} \tag{1}$$

where L, R and M are the stellar luminosity, radius and mass, respectively in solar units. However, to calculate the pre-TP-AGB mass-loss the modified version of the Reimers formula of Schröder and Cuntz 2005 given by:

$$\dot{M} = \eta \frac{LR}{M} (\frac{T_{\rm eff}}{4000{\rm K}})^{3.5} (1 + \frac{g_{\odot}}{4300 g_{\star}}) \tag{2}$$

where $T_{\rm eff}$ is the effective stellar temperature, $g_{\star}$ is the surface gravity of the star in cgs units. Values of 27400cms^{-2} for $g_{\odot}$ and 8.0×10^{-14} for η were adopted (Value recommended by Schröder and Cuntz 2005). This new mass-loss rule appears to give better results for horizonatal branch masses then the Reimer’s rate (Schröder and Cuntz 2005).

This mass-loss law is applied to the variable Y stellar evolution tracks from the Padova stellar evolutionary library (http://pleadi.pd.astro.it) described in detail in Bertelli et al. (2008) and Bertelli et al. (2009). To determine the red giant mass-loss the mass-loss rate was integrated from the beginning of the red giant branch (encoded in the Padova files as brgbs) up to the tip of the red giant branch (encoded as trgb) using the trapezoidal rule. The amount of mass-loss between time steps in the models is given by:

$$\Delta M_i = \frac{1}{2} (\dot{m}_{i+1} + \dot{m}_i)(t_{i+1} - t_i) \tag{3}$$

where t_i and t_{i+1} are the model times and $\dot{m}_{i+1}$ and $\dot{m}_i$ are the mass-loss rates at the corresponding times. The total mass-loss is determined by summing all of the ΔM_is.

Table 1 shows the values of Y and Z for which mass-loss was computed. For all available masses the mass-loss on both the EAGB and RGB was computed. Z is the value of Z on the ZAMS and Y is the value of Y on the ZAMS.

The mass-loss on the RGB as a function of the ZAMS mass for all available values of Y and Z is shown in figure 1. In all panels it is evident the amount of mass-loss decreases as Y increases. This occurs because stars with higher values of Y means the RGB star will have smaller radii and higher surface gravity due to the lower opacity in the outer layers. These factors lower the mass-loss rates and the total mass-loss.

The RGB mass-loss was fit using two linear fits for higher and lower ZAMS masses. The transition point between the fits was determined by visually estimating the mass where the slope appears to change. This mass is typically found around a ZAMS mass of 0.8-0.9 $\mathrm{M}_{\odot}$. The higher mass fit was terminated where the high mass line crosses the horizontal axis. This termination point was also estimated visually. For masses larger the mass where the higher mass fit crosses the axis the mass-loss is 0. The equations of the linear fits for low and high masses are given by $\Delta\mathrm{M}_{\mathrm{RGB,low}}$ and $\Delta\mathrm{M}_{\mathrm{RGB,high}}$. To make the fits work at the two highest metallicities ($Z = 0.008$ and 0.017) the fitting was done by excluding the $\mathrm{M} = 0.6\,\mathrm{M}_{\odot}$ models. These can be safely excluded since the mass-loss for these very low mass stars eliminates their envelope before the tip of the RGB is reached and such models will not be considered in this paper. Visual inspection indicates the fits are in good agreement to the mass-loss calculations.

The equations for $\Delta\mathrm{M}_{\mathrm{RGB,low}}$ and $\Delta\mathrm{M}_{\mathrm{RGB,high}}$ are given by

$$\Delta\mathrm{M}_{\mathrm{RGB,low}} = a_{11}M + a_{10} \tag{4}$$

$$\Delta\mathrm{M}_{\mathrm{RGB,high}} = a_{21}M + a_{20} \tag{5}$$

The mass-loss is found by calculating the value of both ΔMs and finding the maximum value. If the mass-loss is found to be negative then the value of the mass-loss is set to 0. The coefficients of these equations for the different values of Y and Z are shown in table 2.

No attempt has been made yet to calibrate this mass-loss, which will be done in a later paper. However, the mass-loss values from these equations appear to be reasonable. For example a $1.0\,\mathrm{M}_{\odot}$ $Y = 0.26$ $Z = 0.017$ star would experience $0.28\,\mathrm{M}_{\odot}$ of mass-loss on the RGB which is typical of other models. A typical turn-off mass of $0.80\,\mathrm{M}_{\odot}$ with $Y = 0.245$ and $Z = 0.0008$ gives a RGB mass-loss of $0.22\,\mathrm{M}_{\odot}$ which is reasonable giving a zero-age horizontal branch mass of approximately $0.58\,\mathrm{M}_{\odot}$ which is similar to measured values (e.g. Gratton et al. (2010)).

It should be noted, as suggested by the referee, that the method used to find the mass-loss is not consistent with the stellar evolution models. As the star loses mass its surface gravity would decrease causing the star to expand. For the models used this would result in a higher mass-loss rate near the tip of the RGB and a greater amount of mass-loss on the RGB (and the E-AGB) then is calculated here. However, this effect should be relatively small since the deviation will only be really significant at the tip of the RGB. Although the method used here is not strictly consistent the relative differences in mass-loss due to the effect of the ZAMS helium abundances and the ZAMS metallicity should be correct.

2.2 First dredge-up

This is important since when all stars enter the RGB the convective envelope penetrates into regions of the star where partial H burning has occurred bringing these products up to the surface. If a PN is formed this process will have modified the surface abundances. This paper only considers the effects on He and the CNO elements since these are what is observed in planetary nebula. The first dredge-up (FDU) prescription of Groenewegen & de Jong (1994) is used.

2.3 Mass-loss on the early-AGB

The same procedure was applied to the early-AGB (E-AGB) portions of the Padova tracks. An additional condition of starting the mass-loss when the temperature was below 4500K was assumed since this mass-loss law is applicable only to K and M stars.

Figure 2 shows the calculated mass-loss during the E-AGB and the fits to these mass-losses. The most obvious trend is as Y increases so does the amount of mass-loss. This is opposite to the trend on the RGB. In this case the core mass on the AGB is increased which also increases the luminosity. This increase in the luminosity on the E-AGB results in greater mass-loss. This enhancement of mass-loss on the E-AGB is important since it means the higher the value of Y the more mass is lost on the E-AGB. It means such a star has a higher probability to reach the horizontal branch but its envelope may not survive to reach the first thermal pulse.

The mass-loss on the E-AGB is fit using 4 fits in different regions of mass. The lowest mass range ($\mathrm{M} \lesssim 1.5\,\mathrm{M}_{\odot}$) is fit via a cubic, the next mass range up ($1.5\,\mathrm{M}_{\odot} \lesssim \mathrm{M} \lesssim 2.0\,\mathrm{M}_{\odot}$) is fit using a quadratic fit. The next mass range up ($2.0\,\mathrm{M}_{\odot} \lesssim \mathrm{M} \lesssim 4.5\,\mathrm{M}_{\odot}$) is fit using a linear fit. Finally the highest masses are fit using a constant value of mass-loss. The points of intersection between adjacent fits were visually estimated. This procedure gives a good fit to the model mass-losses.

The equations for the E-AGB mass-loss in the first two mass regions are given by:

$$\Delta\mathrm{M}_{\mathrm{E-AGB}} = a_{13}M^3 + a_{12}M^2 + a_{11}M + a_{10} \tag{6}$$

and

$$\Delta\mathrm{M}_{\mathrm{E-AGB}} = a_{22}M^2 + a_{21}M + a_{20} \tag{7}$$

where M is the mass of the star on the ZAMS. Only the coefficients of first two regions have been included in table 3 to save space and since no models of sufficient mass which need the fits for the upper regions are calculated in this paper. The E-AGB mass-loss is calculated by finding the intersection of the two regions and then choosing the appropriate region and plugging into the corresponding equation.

Table 1. Padova Models Used

Z	Y
0.0001	0.23,0.26,0.30,0.40
0.0004	0.23,0.26,0.30,0.40
0.001	0.23,0.26,0.30,0.40
0.004	0.23,0.26,0.30,0.40
0.008	0.23,0.26,0.30,0.40
0.017	0.23,0.26,0.30,0.34,0.40

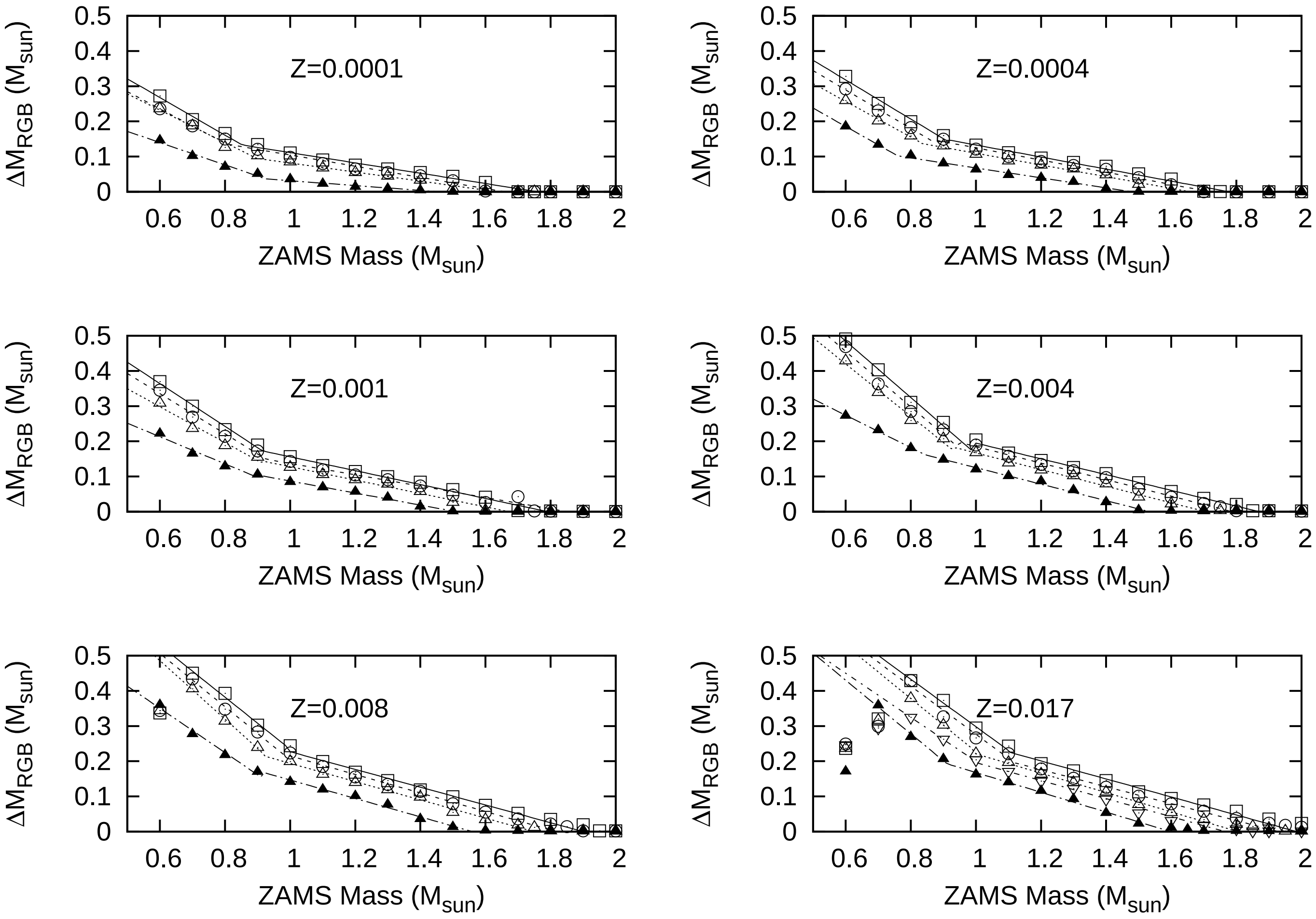

Figure 1. Each panel in the figure shows the calculated mass-loss on the red giant branch for the Z=0.0001, 0.0004, 0.001, 0.004, 0.008 and 0.017 models for different available values of Y. The open squares, open circles, open triangles and closed squares are the mass-losses for Y=0.23, 0.26, 0.30 and 0.40, respectively. The upside down triangles in the Z = 0.017 panel are the mass-losses for the Y = 0.34 models. The solid, dashed, dotted, and dot long dashed lines are the fits for the Y=0.23, 0.26, 0.30, and 0.40 mass-losses, respectively. The dot dashed line is the fit for the Y=0.34 models in the Z=0.017 panel.

2.4 Core mass at the first pulse

From the Padova stellar evolution library I also extracted the core mass as a function of the mass. Figure 3 shows the mass of the carbon-oxygen core as a function of mass for several values of Y and Z. An important point to note is that as the initial helium mass fraction increases so does the mass of the core. The core mass is important since it is the most important factor controlling the luminosity of an AGB star.

Figure 3 show the core mass at the first pulse from the Padova models for Z =0.0001, 0.0004, 0.001, 0.004, 0.008, and 0.017 and Y =0.23, 0.26, 0.30 and 0.40 as a function of mass. Each set of models with a given Y and Z have been fit by a double quadratic fit, one at lower masses $\lesssim 1.5\,\mathrm{M}_{\odot}$ and one at the higher masses. The transition between the two was found between 1.3 and 2.0 $\mathrm{M}_{\odot}$. The transition between the lower mass and higher masses was determined by visual inspection of where the core mass begins to rise steeply. In all cases the fits to the points are good giving core masses which are typically less than $0.02\mathrm{M}_{\odot}$ difference.

The equations of the quadratic fits for low and high

Table 2. Red giant mass-loss coefficients

Y	Z	a_{11}	a_{10}	a_{21}	a_{20}
0.0001	0.23	-0.53375	0.587959	-0.146583	0.257894
0.0001	0.26	-0.48794	0.528645	-0.158946	0.263457
0.0001	0.3	-0.461671	0.509082	-0.128568	0.210224
0.0001	0.4	-0.317215	0.330223	-0.0682917	0.0996025
0.0004	0.23	-0.556562	0.651869	-0.171144	0.304073
0.0004	0.26	-0.54755	0.618164	-0.173845	0.298794
0.0004	0.3	-0.50535	0.560052	-0.166315	0.275781
0.0004	0.4	-0.52254	0.499175	-0.142323	0.210173
0.001	0.23	-0.607168	0.728346	-0.197265	0.353301
0.001	0.26	-0.571589	0.678889	-0.161241	0.298386
0.001	0.3	-0.509972	0.604365	-0.190175	0.317975
0.001	0.4	-0.384763	0.443838	-0.170916	0.258054
0.004	0.23	-0.56752	0.764646	-0.223724	0.418548
0.004	0.26	-0.65305	0.815914	-0.234945	0.419982
0.004	0.3	-0.658095	0.794849	-0.236612	0.403639
0.004	0.4	-0.45996	0.550102	-0.234695	0.359844
0.008	0.23	-0.73907	0.973301	-0.252334	0.479442
0.008	0.26	-0.75636	0.960051	-0.263265	0.478337
0.008	0.3	-0.831625	0.984962	-0.259694	0.453806
0.008	0.4	-0.629659	0.728283	-0.262052	0.40875
0.017	0.23	-0.673745	0.971984	-0.255924	0.50791
0.017	0.26	-0.682876	0.959522	-0.241278	0.465487
0.017	0.3	-0.75486	0.982077	-0.27485	0.495803
0.017	0.4	-0.7626	0.887937	-0.280617	0.448454
0.017	0.34	-0.6274	0.826845	-0.256405	0.452657

Table 3. Coefficients for fits to early-AGB mass-loss

Z	Y	a_{13}	a_{12}	a_{11}	a_{10}	a_{22}	a_{21}	a_{20}
0.0001	0.23	-0.0217193	0.0915006	-0.122712	0.0744702	0.130361	-0.514963	0.508129
0.0001	0.26	-0.215429	0.683192	-0.699251	0.256586	0.0581723	-0.180144	0.136288
0.0001	0.3	-0.00119991	-0.0408501	0.10212	-0.0248815	0.014027	0.0478973	-0.123886
0.0001	0.4	-0.0758491	0.117157	0.0797828	-0.0451725	-0.4921	1.89761	-1.70715
0.0004	0.23	-0.0938861	0.306061	-0.327053	0.139884	0.111841	-0.424637	0.408071
0.0004	0.26	-0.0451582	0.138365	-0.144856	0.0819229	0.0275978	-0.0399283	-0.00915985
0.0004	0.3	-0.0753496	0.168929	-0.0967276	0.044191	0.0182938	0.033923	-0.0942867
0.0004	0.4	0.174151	-0.704201	0.939363	-0.300207	0.2393	-0.69827	0.619354
0.001	0.23	-0.0212184	0.0804842	-0.116847	0.0827674	0.0494489	-0.156333	0.123733
0.001	0.26	-0.0886186	0.296724	-0.336025	0.155924	0.0433492	-0.110378	0.0630566
0.001	0.3	-0.129515	0.334909	-0.262369	0.0984224	0.0160745	0.0320341	-0.0903071
0.001	0.4	0.288478	-1.1637	1.43381	-0.425362	-0.00537448	0.133165	-0.102088
0.004	0.23	0.00637805	-0.00833866	-0.0338022	0.0608243	0.0422666	-0.168079	0.171061
0.004	0.26	0.00369947	-0.00247321	-0.0397723	0.0679063	0.0672259	-0.27111	0.279355
0.004	0.3	-0.0537507	0.173439	-0.212193	0.129599	0.0521944	-0.184787	0.173164
0.004	0.4	-0.689675	1.65297	-1.08412	0.249005	0.0971864	-0.288754	0.274915
0.008	0.23	-0.0179112	0.0872929	-0.148306	0.102219	0.0335246	-0.1486	0.168721
0.008	0.26	-0.00338358	0.0399171	-0.111972	0.103433	0.0289011	-0.120242	0.132401
0.008	0.3	-0.0206433	0.0880253	-0.162452	0.134948	0.0418959	-0.164776	0.172505
0.008	0.4	1.46767	-5.9136	7.68436	-3.10794	0.109614	-0.405738	0.433205
0.008	0.34	-0.012937	-0.00120956	-0.0132868	0.0976855	0.0580864	-0.214707	0.216725
0.017	0.23	-0.00576822	0.041759	-0.106142	0.100898	0.0184395	-0.0922404	0.120053
0.017	0.26	-0.053432	0.248533	-0.399333	0.241192	0.0217703	-0.102463	0.128058
0.017	0.3	0.089118	-0.258045	0.170682	0.042502	0.0213919	-0.0934928	0.113367
0.017	0.4	-0.149333	0.461895	-0.471668	0.256413	0.0343459	-0.145229	0.203376
0.017	0.34	0.399763	-1.37573	1.41367	-0.348366	0.0352993	-0.143105	0.163442

masses are given by $\mathrm{M}_{\mathrm{c0,low}}$ and $\mathrm{M}_{\mathrm{c0,high}}$. The equations are:

$$\mathrm{M}_{\mathrm{c0,low}} = a_{12}M^2 + a_{11}M + a_{10} \tag{8}$$

$$\mathrm{M}_{\mathrm{c0,high}} = a_{22}M^2 + a_{21}M + a_{20} \tag{9}$$

where M is the ZAMS mass. The coefficients for the different values of Y and Z are shown in table 4. The procedure used is to find the point of intersection between the two fits and then to plug in the relevant mass.

The most obvious trend is there is an increase in the core mass as the value of Y increases. This is important since on the AGB a larger core mass leads to a higher luminosity.

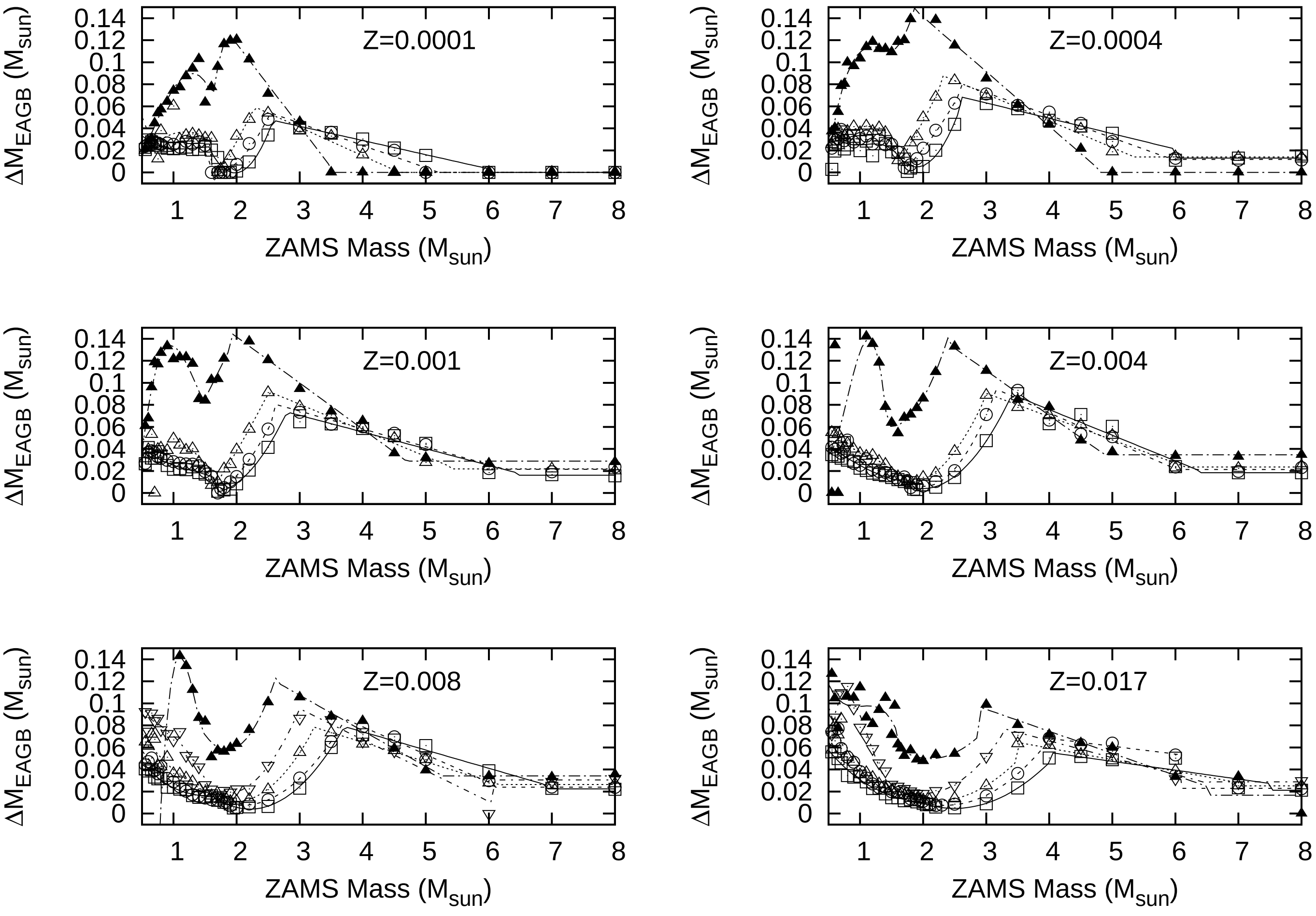

Figure 2. Each panel in the figure shows the calculated mass-loss on the early asymptotic giant branch as a function of ZAMS mass for the Z =0.0001, 0.0004, 0.001, 0.004, 0.008 and 0.017 models for different available values of Y. The symbols and lines have the same meaning as those in figure 1.

This is also important since the mass at the first pulse is an important factor in determining the mass of the CSPN.

2.5 Third dredge up

In synthetic AGB models the standard method to model the third dredge up (TDU) effect is to use a dredge-up parameter λ so that

$$\lambda = \frac{\Delta M_{\rm dredge}}{\Delta M_{\rm c}} \tag{10}$$

where $\Delta M_{\rm dredge}$ is the mass dredged up and $\Delta M_{\rm c}$ is the increase in the core mass during the preceding interpulse phase. During a thermal pulse the star develops a convective shell in the region between the intershell region between the base of the hydrogen-rich envelope and just above the core. This region is helium and carbon rich since it consists of the products of partial helium burning. At the end of the thermal pulse the convective envelope may penetrate into this region and mix this carbon and helium rich material into the envelope. The parameter λ is a measure of how deeply the convective envelope penetrates into this intershell region and determines how much mass is mixed up into the outer layers.

A number of authors have used synthetic models to constrain the value of λ and the minimum core mass value at which TDU can occur, $\mathrm{M_{c,min}}$ (e.g. Groenewegen & de Jong (1993);Marigo, Girardi, & Bressan (1999)). These authors used the LMC and SMC carbon star luminosity functions to constrain both $\mathrm{M_{c,min}}$ and λ parameters. They show the value of $\mathrm{M_{c,min}}$ is approximately $0.58\,\mathrm{M_\odot}$. In this paper the value of $\mathrm{M_{c,min}}$ is treated as a free parameter but values near this are always chosen. The value of λ is a free parameter but it will always be small since most models will experience only one TDU and I expect the value of λ would grow during subsequent thermal pulses if they were to occur.

2.6 Mass-loss on the TP-AGB

On the TP-AGB, mass-loss is calculated by the pulsation period-mass loss law of Vassiliadis and Wood (1993) without their correction for periods above 500 days. To make the transition from the modified Reimer's rate to this pulsation

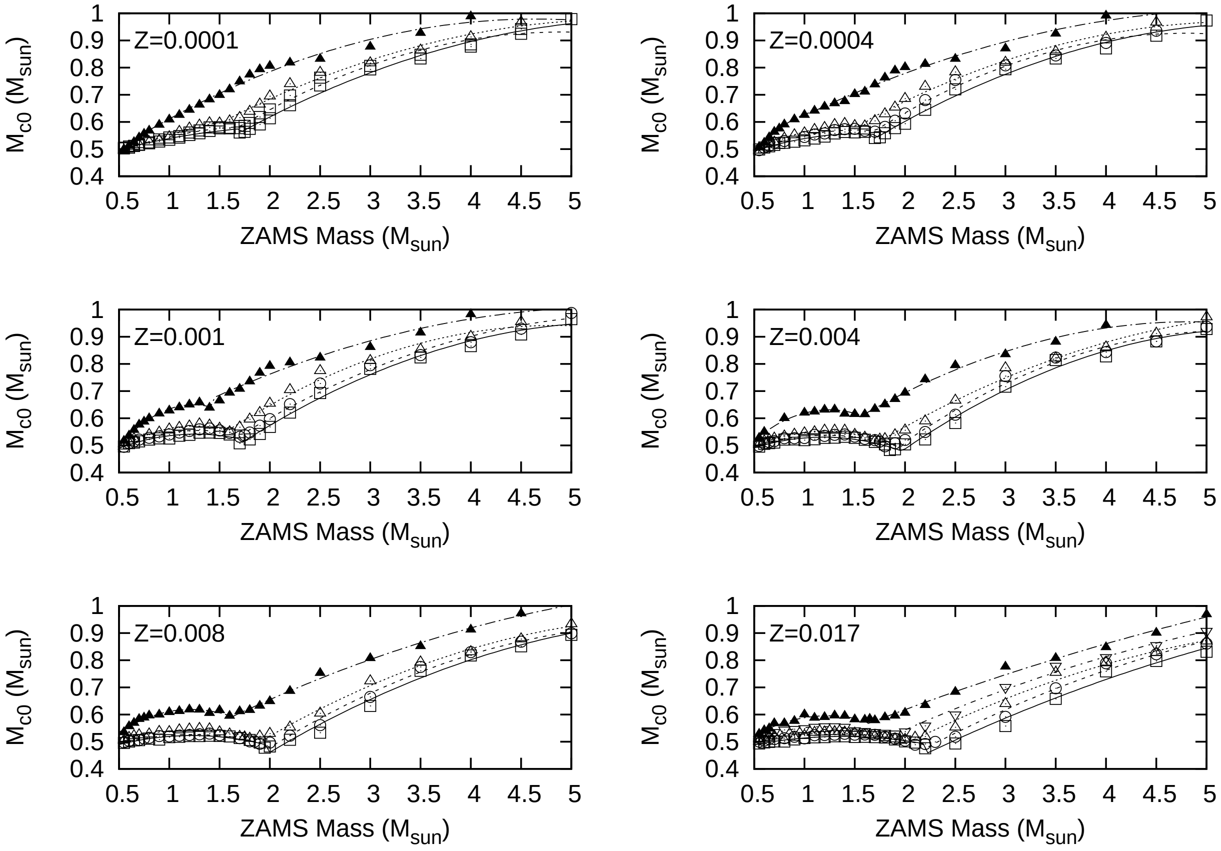

Figure 3. The figure shows the core mass at the onset of the first pulse for the Z =0.0001, 0.0004, 0.001, 0.004, 0.008, and 0.017 models. The symbols have the same meaning as they do in figure 1.

Table 4. Coefficients for the fits to the first pulse core masses

Y	Z	a_{12}	a_{11}	a_{10}	a_{22}	a_{21}	a_{20}
0.0001	0.23	-0.0267946	0.123057	0.442823	-0.0241626	0.283874	0.147144
0.0001	0.26	-0.0449264	0.172855	0.417791	-0.0340353	0.333449	0.114275
0.0001	0.3	-0.0317268	0.175202	0.407754	-0.0236789	0.261573	0.255724
0.0001	0.4	-0.131429	0.4672	0.278697	-0.0276698	0.257098	0.381668
0.0004	0.23	-0.0596658	0.182913	0.415731	-0.0279409	0.313233	0.0872891
0.0004	0.26	-0.0775454	0.235014	0.391988	-0.0373996	0.359006	0.0649862
0.0004	0.3	-0.105043	0.31126	0.357675	-0.0265437	0.282672	0.216724
0.0004	0.4	-0.290637	0.721285	0.197312	-0.0194077	0.213603	0.429181
0.001	0.23	-0.0891579	0.224579	0.400277	-0.0313901	0.344189	0.0106343
0.001	0.26	-0.10291	0.267182	0.381744	-0.0282899	0.320649	0.0719709
0.001	0.3	-0.145894	0.366037	0.342087	-0.0365283	0.353432	0.0866877
0.001	0.4	-0.228835	0.580823	0.28018	-0.020842	0.226895	0.391846
0.004	0.23	-0.0830364	0.196981	0.413575	-0.0364602	0.399655	-0.166655
0.004	0.26	-0.0824008	0.201012	0.414887	-0.039857	0.415317	-0.159354
0.004	0.3	-0.117928	0.279869	0.387053	-0.0250966	0.306343	0.0555899
0.004	0.4	-0.139744	0.34628	0.413321	-0.0323089	0.3129	0.197688
0.008	0.23	-0.0624872	0.153486	0.428388	-0.0240687	0.314676	-0.071922
0.008	0.26	-0.0680031	0.165896	0.425421	-0.0289697	0.34486	-0.0954135
0.008	0.3	-0.0768498	0.187131	0.429621	-0.0256837	0.314658	-0.00601164
0.008	0.4	-0.118314	0.290786	0.436894	-0.0155313	0.224985	0.2672
0.017	0.23	-0.0403038	0.110723	0.443374	-0.0130873	0.233825	0.00316468
0.017	0.26	-0.0494165	0.129165	0.442886	-0.0186948	0.275689	-0.040745
0.017	0.3	-0.0561381	0.142527	0.441254	-0.0198798	0.266728	0.036109
0.017	0.4	-0.10803	0.266918	0.428987	-0.00752814	0.166398	0.315329
0.017	0.34	-0.0844639	0.200431	0.435484	-0.0139933	0.218876	0.161534

mass-loss rule the modified Reimer's rate is used until the pulsation mass-loss rule becomes larger.

2.7 Conditions for formation of a visible planetary nebula

The formation of a visible PN requires that the central star of the planetary nebula (CSPN) reach a temperature of approximately 30000K on its blueward journey from the AGB to the white dwarf cooling tracks before the ejected envelope has sufficient time to disperse into the interstellar medium. In a globular cluster the typical star at the turn-off would produce a CSPN of mass approximately $0.52\,\mathrm{M}_\odot$.

The criteria used in this paper assumes that if a planetary nebula does not form before the ejected envelope expands to 0.5 pc it will not be visible. If an expansion rate of $15\,\mathrm{km}\cdot\mathrm{s}^{-1}$ is assumed for PN then the maximum transition time to form a visible planetary nebula is given by approximately 25000 years. Since PN with expansion ages of 30000 years exist this conservative value is adopted.

To find the approximate transition time for all the $Z = 0.016$ models of Vassiliadis and Wood (1994) were linearly interpolated in time and $\log \mathrm{T}_{\mathrm{eff}}$ to find the time when the effective temperature becomes 30000K. This is the transition time t_{trans}. In figure 4, $\log t_{\mathrm{trans}}$ is plotted as a function of the CSPN mass. The results for the $Z = 0.016$ models are fitted with both a quadratic and cubic fit. These fits are used to extrapolate an approximate range of values for CSPN masses lower than $0.57\,\mathrm{M}_\odot$ cores. Also included were the results from other metallicities. With the exception of one point from the $Z = 0.004$ models (their $\mathrm{M} = 2.0\,\mathrm{M}_\odot$ model) all of the points follow the trend of the cubic.

The quadratic fit is given by:

$$\log t_{\mathrm{trans}} = 19.3316 M_{\mathrm{c}}^2 - 36.0874 M_{\mathrm{c}} + 18.0464 \tag{11}$$

The cubic fit is given by:

$$logt_{\mathrm{trans}} = -181.893 M_{\mathrm{c}}^3 + 417.538 M_{\mathrm{c}}^2 - 322.289 M_{\mathrm{c}} + 85.6 \tag{12}$$

The cubic fit is a better fit in that it passes closer to all the points than does the quadratic fit. The cubic fit seems to better capture the extrapolation, however, since these are used for extrapolation caution needs to be exercised and the values derived here should be treated as approximate. If the transition time is set to 30000 years and the quadratic and cubic equations are solved for M_c the results are $0.522\mathrm{M}_\odot$ and $0.548\mathrm{M}_\odot$, respectively. The cubic extrapolation is weighted more heavily and the adopted minimum value of the CSPN mass to produce a visible PN is $0.545\mathrm{M}_\odot$. This value is very close to the lowest observed value of a globular cluster CSPN central masses, JaFu 1 and JaFu 2. It should be noted a choosing a different set of post-AGB models might lead to different conclusion about the minimum CSPN mass because the transition time in post-AGB models depends strongly on the adapted mass-loss rate.

2.8 TP-AGB models

The TP-AGB is followed using a synthetic AGB code which is a descendent of the Renzini & Voli (1981) code. The code begins with a guess at $\mathrm{T}_{\mathrm{eff}}$ to calculate the surface boundary condition. The equations of stellar structure is then integrated to the base of the convective envelope. The value of the effective temperature is modified until the base of the convective envelope is at the same position as the core mass. The opacities used for high temperatures are the Iglesias & Rogers (1996) and for low temperatures the opacities of Alexander & Ferguson (1994) are used. The luminosity of the star is calculated using the expressions in Wagenhuber & Groenewegen (1998). A mixing length parameter, $\alpha = l/\mathrm{H}_p$, of 1.70 is used. This value is chosen since it is close to typical values of values of α chosen for solar models.

3 RESULTS

3.1 First Generation Star Models

First generation stars are stars with the lowest possible Y of a globular cluster. A series of models with masses between 0.7 and 1.0 $\mathrm{M}_\odot$ were calculated for metallicity values of 0.0002 and 0.004 and a typical Y value of 0.245. Figure 5 shows the final white dwarf mass as a function of the ZAMS mass for a variety of Z values and the Y value of 0.23. If we adopt a typical globular cluster age of $\sim 13\,\mathrm{Gyr}$ it gives typical turn-off masses of $\sim$0.85 $\mathrm{M}_\odot$. Note for all values of the metallicity, Z, the final mass is below the mass needed to produce a visible PN.

If these stars produced visible PNe then there would be a number of PNe in globular clusters with He/H around 0.100 and values of N/O and C/O similar to the values of a typical disk PN. Since the CSPN masses are too low, these models suggest first generation stars do not produce visible PNe as the ejected mass would disperse before it could occur. This reduces the number of expected PNe in GCs since these stars are too low mass to produce them. The larger the fraction of primordial stars is the lower the number of expected PNe. Since no typical PN are observed in the GC system this model explains this observation.

The typical white dwarf mass which would result from these first generation stars is about 0.525 $\mathrm{M}_\odot$. These values are in rough agreement with the typical values inferred for the WD mass at the top of the cooling sequence determined from measurements. Hansen et al. (2007) finds WD masses at the top of the WD cooling sequence of globular cluster NGC 6397 between 0.50 and 0.53 $\mathrm{M}_\odot$ although their error analysis favors a lower value. Hansen et al. (2004) found the mass of the WD at the top of the cooling sequence of globular cluster M4 as 0.55 $\mathrm{M}_\odot$. Strickler et al. (2009) find the mass of the WD cooling sequence of CO WDs in NGC 6397 is 0.53 $\mathrm{M}_\odot$.

3.2 Planetary Nebulae from Second Generation Stars

These stars start on the ZAMS with a high initial He abundance ($Y \approx 0.30$). Figure 6 shows the calculated initial-final relationships for ZAMS stars with masses ranging from 0.7 to 1.0 $\mathrm{M}_\odot$ with $Z = 0.004$ and a range of possible values of Y. It shows as the initial helium abundance is increased the final white dwarf mass increases. This effect is somewhat

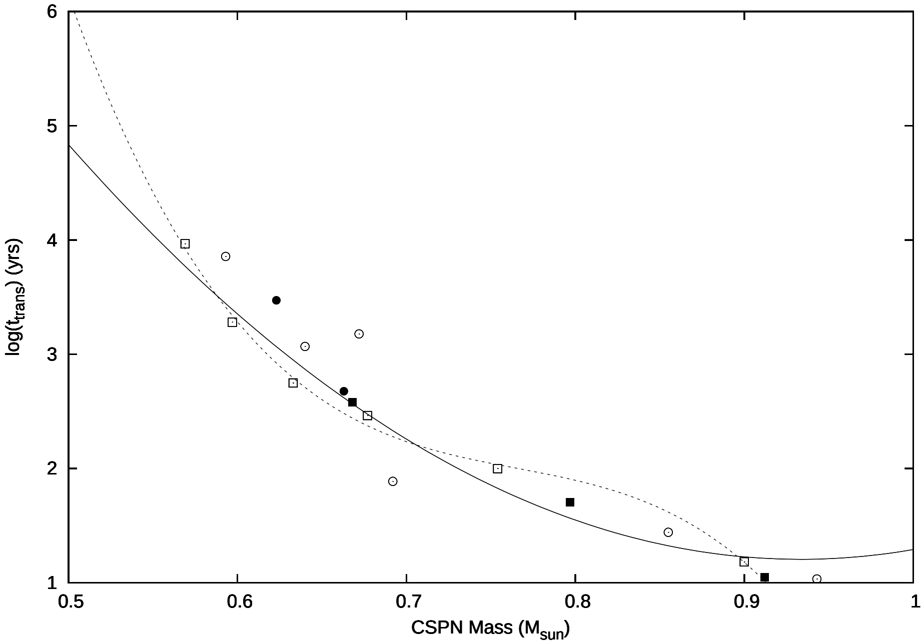

Figure 4. The figure shows the transition times as a function of core mass. The open squares are the results calculated from the Vassiliadis and Wood (1994) $Z = 0.016$ models. The filled squares, open circles and filled circles are the results from the Z =0.008, 0.004 and 0.001 models, respectively. The solid and dashed lines are the quadratic and cubic fits described in the text.

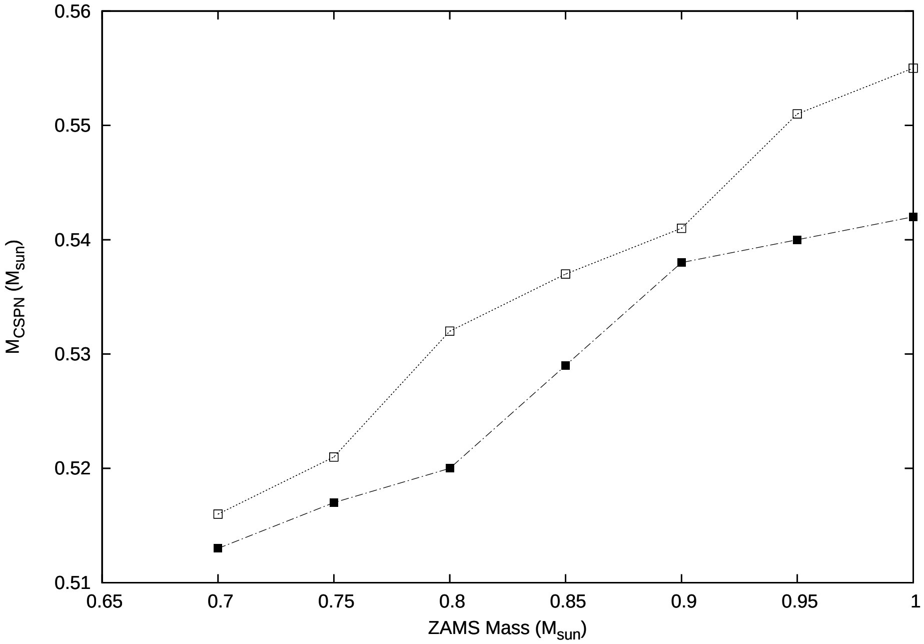

Figure 5. This figure shows the model CSPN masses as a function of ZAMS mass. The open squares are the $Z = 0.0002$ models and the closed squares are the $Z = 0.004$ models.

counter balanced by the shorter ZAMS lifetimes of stars and lower masses of the turn-off with higher initial Y. However even for an assumed turn-off of 0.75 $M_{\odot}$ with the higher values of Y the final mass is near or above the limit to produce a visible PN.

For the stars with a primordial value of helium ($Y =$ 0.245), $Z = 0.004$ and a turn-off mass of 0.85 $M_{\odot}$ the core mass here is 0.529 $M_{\odot}$ which would be too small to produce a visible PN. These models suggest the reason only PN with high He/H appear is this allows larger core masses; which lead to shorter transition times allowing a visible PN to appear.

Since these He enhanced stars can be a significant fraction of the total number of stars in a globular cluster it also predicts that there where two separate populations with different values of Y exist there should should be two CO WD cooling tracks at slightly different masses. Since it appears the typical WD mass is around $0.53\,\mathrm{M}_\odot$ and 0.54-0.55 $\mathrm{M}_\odot$ we estimate that these tracks are separated by 0.01-0.02 $\mathrm{M}_\odot$. This would be observationally challenging to do but might be possible.

Figure 7 shows the model grids used to fit the CSPN masses and He/H for the model parameters which are the closest fit to observed values of M_{CSPN}, He/H and $\log \mathrm{O/H}+12$ from Jacoby et al. of JaFu 1 and JaFu 2. For both nebula the ZAMS values of Z was varied until the model value of O/H was a close match to the observed abundances of O/H found in the nebula (from Jacoby et al.). Then the value of Y was adjusted until a close fit to He/H was obtained. The goal here was to find a reasonable set of parameters and not to fine tune this to the best possible fit.

For JaFu 2 the best fitting model has a core mass of 0.55 $\mathrm{M}_\odot$ which is the same as the observed value. This core mass is produced by a model ZAMS star of mass approximately $0.85\,\mathrm{M}_\odot$ which is a quite reasonable turn-off mass. The values of the model ZAMS Y and Z are 0.282 and 0.00102, respectively. The value of Y is quite reasonable in this case being in line with which are quite reasonably in line with expectations for helium enhancements. JaFu 2 is found in globular cluster NGC 6441 which has an [Fe/H] of -0.46 (Harris (1996 - 2010 edition)), which is a bit higher than the adopted value of Z for the nebula. However, [Fe/H] is not actually fit here and O/H is. It is quite possible there are oxygen depletions which correspond to the helium enhancement here over the different populations in this cluster. This would be similar to what was found by Piotto et al. (2007) for NGC 2808. It is expected He is enhanced by the operation of the CNO cycle which would result in a depletion of oxygen.

For JaFu 1 the best fitting model has a final CSPN mass of 0.54 $\mathrm{M}_\odot$, $Y_{\mathrm{ZAMS}} = 0.333$, $Z_{ZAMS} = 0.006947$. The value of Y is typical of the expected Y enhancements. However the ZAMS mass of the "best" model is $0.70\,\mathrm{M}_\odot$ which is too small but the errors are large enough here to allow a range of possible ZAMS masses up to $0.90\,\mathrm{M}_\odot$. The ZAMS mass of $0.90\,\mathrm{M}_\odot$ gives a core mass of $0.558\,\mathrm{M}_\odot$ which is a little bigger than the observed value from Jacoby et al. (1997) ($0.54 \pm 0.2\,\mathrm{M}_\odot$) but it is well within the error bars.

It is difficult to compare the metallicity of the model for JaFu 1 to that of the cluster Pal 6. A range of potential values are found in the literature. On the low end are the works of Lee & Carney (2002) and Zinn (1985) who find [Fe/H] of -1.08 ± 0.06 and -0.74, respectively. On the high end are the works of Bica et al. (1998) who find $[Z/Z_\odot] = -0.09$ and Ortalani, Bica & Barbuy (1995) and Minniti (1995) who find [Fe/H]=-0.4 and +0.22, respectively. The oxygen abundance of JaFu 1 suggests an overall metallicity between 1/3 and 1/2 solar which is within the metallicity range on the high end of the metallicity possibilities.

The observed nebular mass of JaFu 2 (of $0.04\,\mathrm{M}_\odot$ from Jacoby et al.) is a reasonable match to the models. Low ZAMS mass models with values of Y around 0.30 predict a nebular mass is just a few times $0.01\,\mathrm{M}_\odot$. However, the observed nebular mass of JaFu 1 is much too high ($0.40\,\mathrm{M}_\odot$) but Jacoby et al. determined this using an assumed filling factor of 1 and note a filling factor of 0.1 gives a much lower mass.

These models provide a good fits to the most important parameters; the CSPN mass, the observed value of He/H, the turn-off masses and the oxygen abundance of these PNe. These two nebula can be explained with reasonable progenitors and slightly enhanced values of He/H.

3.3 High C/O Nebula

No star with a mass below the turn-off of any globular cluster will produce a carbon-rich planetary nebula like Ps 1 since a core mass of approximately 0.58 $\mathrm{M}_\odot$ is required for the third dredge-up to occur and since globular cluster stars at the turn-off will have core masses well below this. *There is however a channel to get to these masses - blue stragglers are thought to be merged stars and as such are more massive than stars on the turn-off.* Since blue stragglers in principle could have masses up to twice that of the turn-off these are the most likely channel.

The model used here is the same as discussed in Buell et al. (1997) where after a dredge-up occurs the envelope is so polluted with carbon it is essentially immediately ejected. As discussed by Buell et al. (1997) this single dredge-up heavily pollutes a low metallicity envelope and the metallicity of the envelope jumps to near solar values. This results in an expansion of the star and this resulting expansion causes the star to immediately switch into a superwind phase. The remaining envelope is eliminated in a few thousand years suggesting the carbon star phase would be shorter than the PN phase. This explains the lack of carbon stars in globular clusters.

The models calculated here for low metallicity ($Z \approx 0.0002$) confirm this basic scenario. If $\mathrm{M}_{\mathrm{c,min}}$ is set to $0.57\,\mathrm{M}_\odot$ then the minimum ZAMS mass is $1.15\,\mathrm{M}_\odot$. Figure 8 shows the TP-AGB evolution of the important parameters of this model. On the last pulse the envelope is heavily polluted and note the resulting change in the mass-loss rate. The envelope in this case is ejected in a few thousand years. The model produce a CSPN of the correct mass and the C/O ratio of the model compares favorably to observations of the final ejecta.

Since M15 contains a number of blue stragglers (Yanny et al. (1994)), which, in this model are the progenitor star for a high C/O nebular like Ps 1, M15 is a *reasonable site* for the formation of this PN.

The hardest observation to match is the low nebular mass of Ps 1. In the blue straggler model the predicted nebular mass is $\sim 0.2\,\mathrm{M}_\odot$ whereas the observed nebular mass is about 1/10th this value. The observed smaller nebular mass suggests for the blue straggler model to be a viable model their must have been additional mass-loss, perhaps due to binary interaction. There seems to be no way to reproduce this observation with a single star.

An alternative scenario is described by Otsuka et al. (2008) who argue stars like K648 have evolved from a binary and its progenitor is a CEMP-s star. The problem for this scenario is to match the CSPN mass of K648 the ZAMS mass of the star needs to be larger then the turn-off mass. Otherwise the CSPN mass would be smaller.

Another complication to the model scenario in this pa-

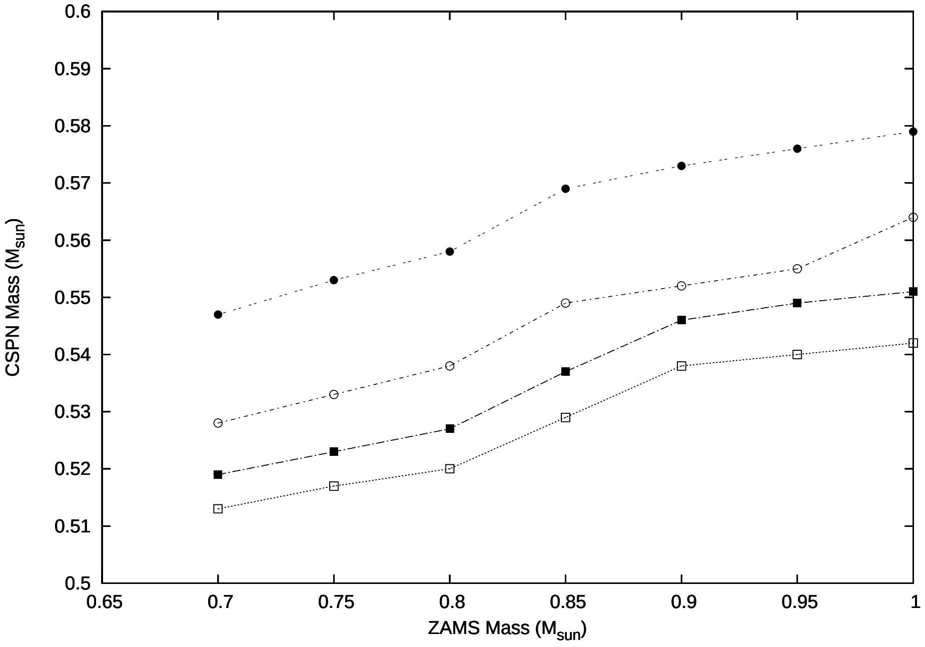

Figure 6. Figure shows the model CSPN masses as a function of ZAMS mass for models with $Z = 0.004$. The open squares, filled squares, open circles, and filled circles are the Y =0.244, 0.274, 0.304, and 0.334 models, respectively.

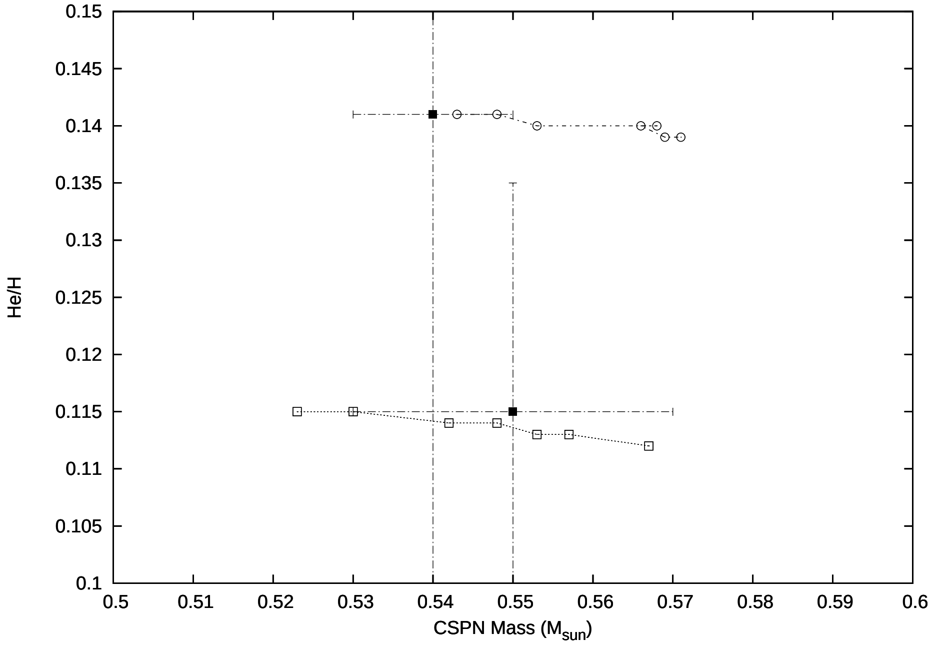

Figure 7. This figure shows He/H as a function of CSPN mass for JaFu 1 and JaFu 2 as filled squares. The models of 'best' fit for JaFu 1 and JaFu 2 discussed in the text are shown as open circles and open squares, respectively. Each of the points on the model curves starts at $0.70\,M_\odot$ and is iterated by $0.05\,M_\odot$ up to $1.00\,M_\odot$.

per is if the initial metallicity of the star is increased the minimum mass to produce a carbon star gets larger. This occurs because the mass of the core at the first pulse gets smaller with smaller metallicity. This is consistent with studies which infer the minimum mass to produce a carbon star in the SMC, LMC and the Galaxy where as the metallicy goes up so does the minium mass (See - references here (Marigo, Groenewegen, etc.)). In this model a blue straggler in a higher metallicity cluster ($Z = 0.004$) would be less likely to produce a carbon-rich nebula. This blue straggler would produce a visible PN with an oxygen-rich composition.

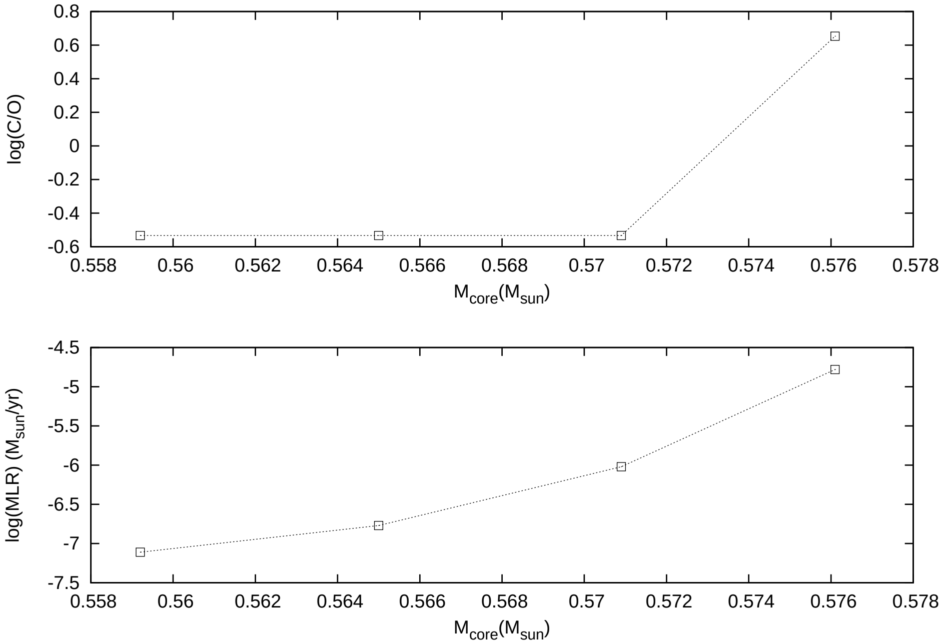

Figure 8. This figure shows the TP-AGB evolution of a ZAMS star M=1.15 $M_\odot$, $Z = 0.0002$ and $Y = 0.2454$. The top panel shows the evolution of the ratio of carbon to oxygen. The lower panel shows the evolution of the mass-loss rate (MLR). The points are the values at the end of each interpulse cycle.

Blue stragglers are rare but prominent members of GCs and cannot be expected to produce many PNe. A simple estimate can be obtained in the following manner; assume the average lifetime of a blue straggler is 10^9 years and the lifetime of a PN is 25000 years. If it is assumed every blue straggler produces a PN then we should expect 1 PN for every 40000 blue stragglers. If we assume the number of blue stragglers per cluster is 100-200 and use 150 for the number of globular clusters then the total number of blue stragglers in the GC system should be between 15000-30000. This would give the number of PN from this channel as 0.375-0.70 PNe. The assumed numbers are probably optimistic since the lifetime of blue stragglers could be larger; the lifetime of PN smaller and the 100-200 is the number of blue stragglers for bigger clusters. The actual number of expected PN may be even smaller. If it is assumed there are sufficient numbers to produce only one in the entire GC system then it is possible Ps 1 is the only example and an oxygen-rich PN is equally likely.

This model shows it is possible to produce carbon-rich PNe in globular clusters but it is not possible for it to match the nebular mass of Ps 1, which can only be done by invoking an ad hoc binary explanation. This may be reasonable since this star probably formed in a binary but at the moment it is untestable since there are no similar PN in the GC system to compare it to. A similar PN with a well constrained CSPN mass and nebular mass would tell us if K648 is typical of its class. The only possible known analogs are the halo PN such as BB-1 and H4-1 which have C/O>1 (see Howard et al.). Unfortunately the distances to these nebula is poorly known and it will be difficult to get precise information about the CSPN and nebular masses for comparison purposes.

3.4 What is the origin of the planetary nebula in M22?

M22 contains a very interesting PN GJJC-1 which is nearly hydrogen free (Gillett et al. 1989) because no nebular hydrogen lines have been detected. The nebula appears to be overabundant in O and Ne. The central star of GJJC-1 has been observed (Harrington and Paltoglou 1993) and it is suggested that the surface abundances are He/H=0.5, C is 6 times solar and N is 14 times solar (Harrington and Paltoglou (1993), Rauch et al. (1998)).

There are only two other hydrogen free nebula out of approximately 1000-2000 total known in the Galaxy. Given the inferred percentage of a PN being hydrogen free of 0.1-0.2 percent it seems unlikely that this PN simply occurred by chance. One speculative possibility is the existence in some clusters of a third generation of stars which would have very extreme ($Y = 0.40$) helium enhancement.

Recent work on the cluster by Da Costa et al. (2009) and Marino et al. (2009) indicates M22 has at least two separate populations which vary in their value of [Fe/H]. The average [Fe/H] is between -1.7 and -1.9 but it ranges up to -1.4. The higher [Fe/H] population probably has a higher value of Y. It has been suggested M22 is the remains of a captured dwarf elliptical galaxy. As such it seems a reasonable candidate for a population with extreme helium enhancement. M22 may also have a more complicated star formation history with the formation of different populations spaced out by significant amounts time.

A model with $M = 0.80\,M_\odot$, $Y = 0.40865$, and $Z = 0.000886$ was run. In this model the star reached the horizontal branch but the entire envelope was lost by the end of the E-AGB. The mass-loss on the E-AGB increases as the value of Y goes up because the core mass goes up. The luminosity of an AGB star will depend strongly on the core mass and this increased luminosity drives the increased mass-loss. This model produces a core mass of $0.60\,\mathrm{M}_\odot$. If the mass is lowered to $0.75\,\mathrm{M}_\odot$ then the model once again produces a HB star but all the remaining envelope mass is lost on the E-AGB. This lower mass produces a $0.58\,\mathrm{M}_\odot$ remnant.

Why is this significant? This is close to the inferred mass of GJJC-1's CSPN and production of a hydrogen free nebula requires getting rid of the initial hydrogen before the PN phase. Getting rid of all the envelope means if this star experiences a thermal pulse then there would be little to no hydrogen ejected and the star would eject helium rich material and it would look much like GJJC-1. This suggestion should be regarded as speculative and the positive evidence for it is thin but the idea seems to be possible and merits additional study.

3.5 How many of each type?

Without a detailed population study which is beyond the scope of this paper it is only possible to show the numbers work out approximately correct. I start by assuming the Jacoby et al. (1997) statement that given the total luminosity of the GC system then the number of PNe should be 16. If it is assumed that 70 percent of globular cluster stars are primordial and have a turn-off in the 0.80-0.90 $\mathrm{M}_\odot$ range then this reduces the number to about 4-5 since these stars produce none. The number from this appears to be 3 which is in rough agreement. Further, assuming all blue stragglers produce a visible PN, we assume about 1 from this part which matches the designation of Ps 1 (K648) as being produced by this channel. The rest will be produced by second generation stars (which may or may not all produce a visible PN). Therefore the numbers are roughly consistent with the number of known PNe.

4 DISCUSSION

What do JaFu 1 and JaFu 2 tell us about second generation GC stars? They confirm, independently of the use of colour magnitude diagrams, stars exist in globular clusters with $Y = 0.28 - 0.33$ and it suggests these second generation stars are a significant fraction of the number of GC stars. These two PNe could turn out to be very important since they allow the direct observation of elements which can not be observed directly using stellar spectroscopy.

For JaFu 1 $\log\mathrm{N/O} = -0.52$ (Jacoby et al.) which is slightly higher than $\log\mathrm{N/O}_\odot = -0.88$ (Asplund, Grevesse, & Sauval 2005). This ratio is consistent with both a first dredge-up event and possibly a small amount of nitrogen enrichment or oxygen depletion. For JaFu 1 $\log\mathrm{S/O} = -1.35$ which is consistent with the solar $\log\mathrm{S/O} = -1.50$. From these abundance ratios either all these have been enriched by the same relative amount or the star has not been enriched relative to a first generation star in Pal 6. The sulfer abundance of JaFu 1 is given by $\log\mathrm{S/H} - \log\mathrm{S/H}_\odot = -0.55$. This is consistent with a cluster with metallicity between 1/3 and 1/2 solar. If the cluster's metallicity is on the lower end of its range then this would indicate all elements have been enhanced in this cluster.

JaFu 2 may indicate a depletion of oxygen in NGC 6441. The value of $\log\mathrm{O/H} - \log\mathrm{O/H}_\odot = -0.93$ and the value of $\log\mathrm{Ar/H} - \log\mathrm{Ar/H}_\odot = -0.72$. Since this is a lower metallicity cluster we would expect oxygen as an alpha element to be enhanced however it appears to be less enhanced relative to argon. This would be consistent with the enhanced material having been processed by CNO cycling.

As GCs age they leak stars into the field via collisions and also by tidal stripping. In fact it is estimated that 4-9% of halo stars are 2nd generation globular cluster stars (Vesperini et al. 2010). If second generation halo stars become halo stars they could produce PN similar to JaFu 1 and JaFu 2 and may be GJJC-1. However, this is a small fraction of the halo stars and it is quite possible no such star has been observed.

Other places to look for similar PN might be the system of satellite galaxies. The GCs ω Centauri, M54 and M22 are all possible captured satellite galaxies and all of them have multiple populations (see Piotto 2009). This suggests multiple populations might be common in satellite galaxies and this model predicts there may be PNe in these satellite galaxies similar to the GC PNe.

5 CONCLUSIONS

This paper presents a series of models for the expected TP-AGB stars in globular clusters. The results of these models are compared to the observed abundances of the globular cluster PNe and the measured masses of WDs.

(i) These models suggest the typical unenriched ZAMS star at the turn-off will not produce a visible PN, which explains small number of PN in GC. The CSPN mass is too small to produce a visible PN during the transition from the AGB to the white dwarf phase.

(ii) The PNe JaFu 1 and JaFu 2 are consistent with being produced by second generation stars in the globular cluster. Both have He/H ratios which are consistent with $Y_{\mathrm{ZAMS}} \approx 0.30$ which is consistent with results for second generation stars from fitting colour-magnitude diagrams to the cluster.

(iii) Due to its large core mass (0.56-0.58 $\mathrm{M}_\odot$) it is quite possible the PN GJJC-1 is consistent with a third generation ($Y \approx 0.40$) progenitor.

(iv) The nebula and central star Ps 1 and K648 respectively may have been produced from a blue stagger. However, this interpretation is in doubt since the nebular mass of Ps1 is too small to be explained by this model. The high CSPN mass favors this hypothesis but the low nebular mass does not favor it. Additional mass-loss due to binary interaction could explain this.

(v) This model suggests that there should be, in globular clusters with different populations with different helium abundances, two white dwarf cooling tracks with the second generation star with higher Y producing a slightly more massive WD then the first generation star with a lower Y.

ACKNOWLEDGMENTS

REFERENCES

Alexander D.R. and Ferguson J.W. 1994, ApJ, 437, 879

Alves D.R., Bond H.E. & Livio M. 2000, AJ, 120, 2044

Asplund M., Grevesse N., Sauval A.J., 2005, in ASP Conf. Ser. 336, Cosmic Abundances as Records of Stellar Evolution and Nucleosynthesis, ed. F.N. Bash & T.G. Barnes

Bedin L.R., Piotto G., Anderson J., Cassisi S., King I.R., Momany Y. and Carraro G. 2004, ApJ, 605, L125

Bica E., Claria J.J., Piatti A.E. & Bonatto C., 1998, A&AS, 131, 483

Bertelli G., Girardi L., Marigo P., and Nasi E. 2008, A&A, 484, 815

Bertelli G., Nasi E., Girardi L. and Marigo P. 2009, A&A, 508,355

Bianchi L., Bohlin R., Catanzaro G., Ford H., Manchado A. 2001, AJ 122, 1538

Bianchi L., Ford H., Paresce F., De Marchi G. 1995, A&A, 301,537

Buell J.F., Henry R.B.C., Baron E., Kwitter K.B., 1997, ApJ, 483, 837

Buell J.F., 1997, PhD thesis, Univ. Oklahoma

Caloi V., D'Antona F. 2007, A&A, 450,523

Calamida A., et al. 2008, ApJ, 673, L23

Carretta E., et al. 2009, A&A, 505, 117

Da Costa G.S., Held E.V., Savianne I. and Gullieuszsk M. 2009, ApJ, 705, 1481

Davies M.B., Piotto G., Angeli F.D. 2004, MNRAS, 349, 129

Cool A.M., Piotto G. and King I.R. 1996, ApJ, 468, 655

Gavilan M., Buell J.F., Molla, M., 2005, A&A, 432, 861

Gillett F.C., Jacoby G.H., Joyce R.R., Cohen J.G., Neugebauer G., Soifer B.T., Nakajima T., Matthews K. 1989, ApJ, 338, 862

Gratton R.G. et al. 2001, A&A, 369, 87

Gratton R.G., Carretta E., Bragaglia A., Lucatello S. & D'Orazi V. 2010, A&A, 517, 81

Groenewegen M.A.T. and de Jong T., 1993, A&A, 267, 410

Groenewegen M.A.T. and de Jong T., 1994, A&A, 283, 463

Hansen B.M.S., et al., 2002, ApJ, 574, L155

Hansen B.M.S., et al., 2004, ApJS, 155, 551

Hansen B.M.S., et al., 2007, 671, 380

Harrington J.P. and Paltoglou G. 1993, ApJ, 411, L103

Harris W.E. 1996, AJ, 112, 1487

Howard J.W., Henry R.B.C., McCartney S. 1997, MNRAS, 284, 465

Iglesias C.A. and Rogers F.J. 1996, ApJ, 464, 943

Jacoby G.H., Morse J., Kellar L., Kwitter K.B., Henry R.B.C 1997, AJ, 114, 2611

Lee J.-W. & Carney B., 2002, AJ, 123, 3305

Marigo P., Girardi L., Bressan A., 1999, A&A, 344,123

Marino A.F., Milone A.P., Piotto G., Villanova S., Bedin L.R., Bellini A. and Renzini A. 2009, A&A, 505, 1099

Milone A.P., Piotto G., Bedin L.R., Marino A.F., Momany Y., and Villanova S. 2010, Mem. S.A.It

Milone A.P., Piotto G., Bedin L.R., Bellini A., Marino A.F., and Momany Y. 2010, in Proceedings SF2A 2010, 319, eds: S. Boissier, M. Heydari-Malayeri, R. Samadi, and D. Valls-Gabauds

Minniti D., 1995, A&A, 303, 468

Ortalani S., Bica E., & Barbuy, B., 1995, A&A, 296, 680

Otsuka M., Izumiura H., Tajitsu, A., Hyung, S. 2008, ApJ, 682, L105

Peña M., Torres-Peimbert S. and Ruiz M.T. 1992, A&A, 265, 757

Piotto G. et al. 2007, ApJ, 661, L53

Piotto G., 2009, in Proceedings IAU Symposium 258, 233, eds. E.E. Mamajek, D.R. Soderblom, R.F.G. Wyse

Rauch T., Dreizler S., Wolff B. 1998, A&A, 338, 651

Rauch T., Heber U., Werner K. 2002, A&A, 381, 1007

Reimers D. 1975, Mem. Soc. R. Sci Liège, 8, 369

Renzini, A. 1979, in Stars and Systems, ed. B.E. Westerlund (Dordrecht: Reidel), p. 155

Renzini A. & Voli M. 1981, A&A, 94, 175

Renzini A., et al., 1996, ApJL, 465, 23

Richer H.B., et al., 1997, ApJ, 484, 741

Schröder K.P., Cuntz M., 2005, ApJ, 630, L73

Strickler, R.R., et al. 2009, ApJ, 699, 40

Vassiliadis V.W., Wood P.R., 1993, ApJ, 413, 641

Vassiliadis V.W. & Wood P.R., 1994, ApJS, 92, 125

Vesperini E., McMillan S.L.W., D'Antona F., D'Erocle A., 2010, ApJ, 718, 112L

Wagenhuber J., Groenewegen M.A.T., 1998, A&A, 340, 183

Yanny B., Guhathakarta P., Bahcall J.N., Schneider D.P., 1994, AJ, 107, 1745

Zinn R., 1985, ApJ, 293, 424

Zoccali, M., et al. 2001, ApJ, 553, 733